

RESEARCH PAPER

## Antimicrobial Activity of Silver Nanoparticles (AgNPs) on Biofilm Formation for Pathogenic Bacteria Isolated from UTI of Iraqi Patients

Tariq Saddam Tariq <sup>1\*</sup>, Ashwak Jasim Kzar <sup>2</sup>, Hussam Sami Awayid <sup>3</sup>

<sup>1</sup> Al-Musayyib General Hospital, Babylon, Iraq

<sup>2</sup> College of health and medical technology, Middle technical university, Baghdad, Iraq

<sup>3</sup> Suwaira Technical Institute, Department of Medical Laboratory Techniques, Iraq

### ARTICLE INFO

#### Article History:

Received 06 August 2024

Accepted 28 September 2024

Published 01 October 2024

#### Keywords:

Biofilm

Pathogenic Bacteria

Silver Nanoparticles

Urinary Tract Infection

### ABSTRACT

Urinary tract infections (UTIs) are one of the most common infectious diseases. Silver nanoparticles (AgNPs) are widely used due to their antimicrobial and antibiofilm activities. In the current study, 75 urine samples were collected from patients with urinary tract infection (UTI), with their ages ranging from (10-85) years, who visited Al-Musayyib general hospital and Alexandria general hospital/Babylon province during the period from 2<sup>nd</sup> January to 14<sup>th</sup> February 2024. All the urine samples were subjected to standard bacteriological processes and characterized based on their culture morphology and microscopic examination, as well as the biochemical tests. AgNPs were prepared by chemical methods and characterized via fourier transform infrared spectroscopy (FTIR), Zeta potential (ZP), scanning electron microscope (SEM) and transmission electron microscope (TEM). Well-diffusion was used to screen the antimicrobial effects of AgNPs on the six isolated bacteria *Escherichia coli*, *Klebsiella pneumonia*, *Pseudomonas aeruginosa*, *Proteus mirabilis*, *Staphylococcus aureus* and *Enterococcus faecalis*. Minimal-bactericidal concentrations (MBC) of AgNPs were determined to study their antibiofilm effect at minimum-inhibitory concentrations (MIC). The highest urinary tract infection rate was shown to be with *Klebsiella pneumonia* (25.33%) followed by *E. coli* (22.67%), while the lowest infection rate was with *Enterococcus faecalis* (6.67%). and result Showed that all isolates were strong biofilm producers. Exposure of the isolates to the AgNPs resulted in pronounced inhibition zones and reduced biofilms at (MIC) values. These results indicate that AgNPs with an aptitude to disrupt biofilm development for pathogenic bacteria strains it caused UTI.

### How to cite this article

Tariq T., Kzar A., Awayid H. Antimicrobial Activity of Silver Nanoparticles (AgNPs) on Biofilm Formation for Pathogenic Bacteria Isolated from UTI of Iraqi Patients. J Nanostruct, 2024; 14(4):1067-1076. DOI: 10.22052/JNS.2024.04.008

### INTRODUCTION

Urinary tract infections (UTIs), a common urologic condition that affects millions of individuals worldwide, are caused by bacteria that are extremely resistant to antimicrobials [1]. Most hospital admissions throughout the world are due to urinary tract infections (UTIs), which

are a severe health issue and have comorbidities in patients with underlying conditions. In those without anatomical or functional problems, UTIs typically go away on their own, although they tend to come back [2]. Bacterial biofilms, an aggregate of microorganisms, are mainly responsible for persistent infections leading to recurrences and

\* Corresponding Author Email: [edc0072@mtu.edu.iq](mailto:edc0072@mtu.edu.iq)



increased tolerances to major drug treatment. Bacterial biofilm formed on medical devices such as urinary catheters cause severe problems for patients and affects the implants' function. UTI associated with microbial biofilms developed on catheters in hospitalized patients is the most common. Thus, an urgent need for novel approaches and strategies for using an antimicrobial agent to inhibit biofilm formation is highly required [3].

Silver nanoparticles represent the common antimicrobial agent. Due to recent technological advancement [4], silver nanoparticles have resurfaced in the medical field. Because of their low toxicity to mammalian cells and stronger antimicrobial activity, silver nanoparticles have been used in a variety of disciplines. Silver nanoparticles are utilized for the treatment of biofilms associated with medical devices that threaten life [5].

At these days nanoparticles (NPs) are used as antibacterial due to it have chemical-physical addition to biological effect. A big group of microbial cells adhering to a surface are called biofilm. Exposure to nano particles such as (Ag, Al<sub>2</sub>O<sub>3</sub>, Ni) may prevent colonization of new bacteria onto the biofilm [6]. By decreasing the size of the silver particles to the nanoscale, the antibacterial and anti-biofilm activities of the silver were increased as the surface area of the particles increased. As a result, the level of Ag<sup>+</sup> release is greater than that of silver particles in their elemental form. Consequently, silver nanoparticles have a better ability to adhere, penetrate, and aggregate inside the cell membrane of bacteria, resulting in a large amount of silver ions being released within the cell. The presence of water channels all over the biofilm could explain silver nanoparticles biofilm inhibitory action. These pores were important in nutrient transport, and silver nanoparticles could pass right through these pores and reveal their antibacterial action [7].

The aim of this study was to evaluate the antibacterial activity of silver nanoparticles against biofilms formed by bacterial isolates causing UTI.

## MATERIALS AND METHODS

Collection and identification of bacterial isolates: In the current study, 75 urine samples were collected from patients with urinary tract infection (UTI), with their ages ranging from (10-85) years, who visited Al-Musayyib general

hospital and Alexandria general hospital/Babylon province during the period from 2<sup>nd</sup> January to 14<sup>th</sup> February 2024. All the urine samples were subjected to standard bacteriological processes and characterized based on their culture morphology and microscopic examination, as well as the biochemical tests. Identification of the clinical isolates were confirmed via the automated Vitek-II system (Biomerieux, France).

AgNPs were prepared by chemical methods via using 4mM of silver nitrate, 0.4mM tri-sodium citrate dehydrates as a reducing agent, and 0.5mM sodium dodecyl sulphate-SDS as a capping agent. Silver nitrate was dissolved in 100 ml of deionized water under hot plate magnetic stirring until it reached 80C. A mixture of tri-sodium citrate dehydrate and SDS was also dissolved in 100 ml of deionized water, and was dropped for 30 minutes under continuous stirring. The final mixture was kept at 80oC, 350 rpm, for two hours. Changing the color to yellow indicates the AgNPs' formation, and then it was cooled at room temperature, stored in a dark place in a refrigerator [8].

The resultant silver nanoparticles were characterized by Fourier-Transform Infrared Spectroscopy (FTIR), zeta potential, scanning electron microscope (SEM) and transmission electron microscope (TEM).

To show their effects on the pathogenic bacteria, four concentrations of AgNPs were prepared 30 µg.mL<sup>-1</sup> AgNP, 50 µg.mL<sup>-1</sup> AgNP, 90 µg.mL<sup>-1</sup> AgNP, and 110 µg.mL<sup>-1</sup> AgNP. Well-diffusion method was used to test the antibacterial effect on different nanoparticles. Five wells were punched into the agar using a sterilized well cutter. The wells were loaded with 80µl of different concentrations of 4mM AgNP (30, 50, 90 and 110) µg.mL<sup>-1</sup> of the AgNP solution for all types of bacteria, deionized water was used as a controlling factor. The dishes were incubated at 37C° for 24 hours. Results were obtained by measuring the inhibition zone [9]. Three replicates were made for each treatment.

Minimum inhibitory concentration (MIC) and minimum bactericidal concentration (MBC) were determined as follows: Test tubes containing 0.8 mL of BHI broth were added with 0.1 mL of a suspension of the bacteria used in the study, along with 0.1 mL of AgNPs at various concentrations (30, 50, 90, or 110 µg.mL<sup>-1</sup>). These test tubes were then compared to 0.5 McFarland standard tubes. Before turbidity readings were taken, the tubes were given a vigorous shake and left at 37C° for

24 hrs. Afterward, turbidity was used to record the results. 100 l of the mixture was then spread out in a loop on MHA medium and incubated for 24 hrs. at 37 C°. The results were then recorded based on whether or not growth appeared on the agar [10].

Static biofilm analysis: The biofilm formation wells of the identified strains was examined via microtiter plate assay. Concisely, overnight cultures of the selected bacteria were added into the cavities of the microplate (MTP, Cito-test Labware, China) containing sterilized brain heart broth (BHB, Neogen, USA) enriched with 2% glucose. As control, wells housing BHB were employed. Following the 24 hours of incubation of the inoculated microplate in a static state, the wells were cleared from the supernatant and washed threefold with sterilized phosphate buffer-saline (PBS). Then, the wells of the MTP were stained via 1% crystal-violet solution and rinsed gently threefold with PBS to remove excess dye. Once dried, the wells were supplemented with 95% ethanol solvent to spectrophotometrically measure the produced biofilms at a wavelength of 630 nm via Elisa (Bio-Tek Instruments, USA).

Most potent biofilm developers were hand-picked to analyze the antibacterial activity of the AgNPs [11].

Anti-biofilm impact of nanoparticles: The competency of the chemical nanoparticles to inhibit biofilm development at MIC was assessed against a selection of 6 strongest biofilm producer pathogenic strains. In brief, 200µL of sterile BHB enriched with 2% glucose was added into the wells of flat-bottom MTP. Then, 15 µL from the MIC wells were added into the wells and incubated overnight at 37 °C under a static state. For control, wells with bacterium inoculum and BHB solely were considered. Liquid cultures were removed from the wells after incubation, followed by three PBS rinses and 1% crystal violet staining. After the staining process, PBS was employed to rinse the excess dye from the wells, 95% ethanol solution was used for elution and an ELISA reader at the wavelength of 630 nm was considered for quantification of the formed biofilms. [11]. Classification of bacterial biofilm formation by tissue culture plate method in to three categories: Weak (BF <0.123),Moderat(0.123> BF ≤0.345),

Table 1. Distribution of UTI patients according to microorganism type.

Name of isolated bacteria	No.	Percentage
<i>E.coli</i>	17	(22.67%)
<i>Klebsiella pneumonia,</i>	19	(25.33%)
<i>Pseudomonas aeruginosa</i>	16	(21.33%)
<i>Proteus merabilis,</i>	9	(12%)
<i>Staphylococcus aureus</i>	9	(12%)
<i>Enterococcus faecalis</i>	5	(6.67%)
Total	75	(100%)

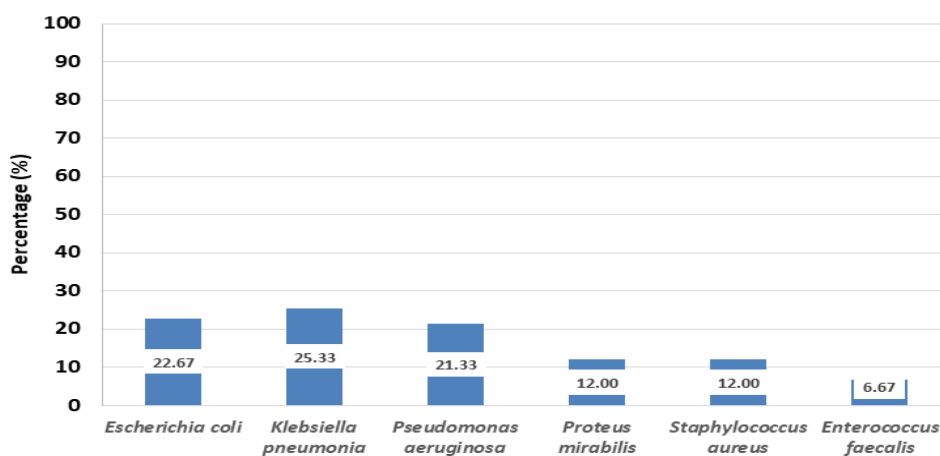


Fig. 1. Distribution of isolates according to microorganism type.

and Strong (BF >0.345) at OD. value 630 nm.[12] Data are documented as removing completely and incompletely in the biofilm bacterial growth with presence of AgNPs nanoparticles and compared with the absence of AgNPs nanoparticles (control).

### RESULTS AND DISCUSSION

In the current study, sample distribution according to microorganism type showed that 17 (22.67%) isolates were *E.coli*, 19 (25.33%) isolates were *Klebsiella pneumonia*, 16 (21.33%) isolates were *Pseudomonas aeruginosa*, 9 (12%) isolates were *Proteus merabilis*, 9 (12%) isolates of *Staphylococcus aureus* and 5 (6.67%) isolates of *Enterococcus faecalis*, as shown in Table 1 and

Fig. 1.

The final mixture was kept at 80°C, 350 rpm, for two hours. Changing the color to yellow indicates the AgNPs' formation. And then it was cooled at room temperature, stored in a dark place in a refrigerator (Fig. 2).

Characterization of silver nanoparticles A: show transmission electron microscope (TEM) (Zeiss, Germany) used to identify the morphological feature of the silver nanoparticles, show a size range of 10 to 50 nm [13] and B: show Field Emission Scanning Electron Microscope (FE-SEM) analysis was used to study the particle's size, AgNPs shape, and surface morphology by scanning electron microscope (Zeiss, Germany) show a size



Fig. 2. AgNO<sub>3</sub> (white) and AgNP (yellow) solutions.

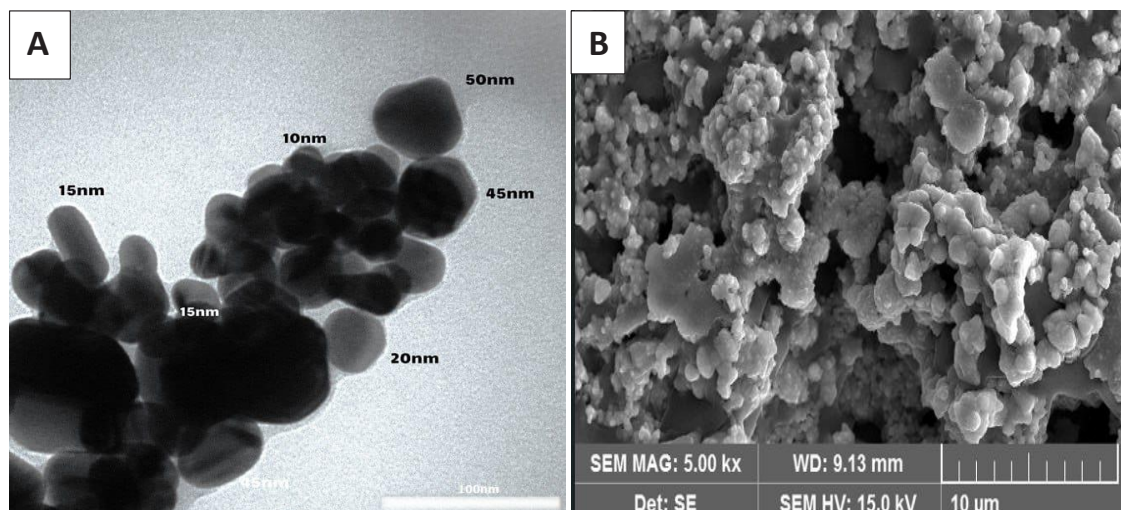


Fig. 3. Characterization of silver nanoparticles A: transmission electron microscope (TEM) B: Scanning Electron Microscope (SEM).

10 μm, at a magnification power of 50.00KX, with working distance 9.13mm with high voltage 15.0 KV [14] as shown in Fig. 3 (A,B).

Fig. 4A show the zeta potential which was also measured and in the current study the presence of negatively charged AgNPs with a zeta potential (-17.2 mV) was confirmed by zeta potential measurement [15]. Zeta potential affects nanoparticle adsorption unto a surface as well as its ability to permeate membranes therefore can be used for predicting emulsion instability. The zeta potentials of nanoparticles can also indicate how well it can fight aggregation [16] and Fig. 4B show fourier transform infrared spectroscopy (FTIR) spectra of AgNPs NPs. Peaks at 3450.65 cm<sup>-1</sup> matching to stretching vibration of O-H bond and peaks showed at 2873.94 cm<sup>-1</sup> matching to the C-H stretching vibrations. The peaks at 1653.00 cm<sup>-1</sup> and 1560.41 cm<sup>-1</sup> and 1473.62 cm<sup>-1</sup> corresponds to the C=O vibrations and with peaks 1319.31 cm<sup>-1</sup> and 1271.09 cm<sup>-1</sup>, C-C and C-N stretching and with peaks 1066.64 cm<sup>-1</sup> O-H stretching observation of

peaks at 898.83 cm<sup>-1</sup> and 773.46 cm<sup>-1</sup> and 609.51 cm<sup>-1</sup> and 505.35 cm<sup>-1</sup> and 426.27 cm<sup>-1</sup> corresponds to Ag NPs [17] .

The data in Table 2 and Fig. 5 revealed that antibacterial activity of 30 μg.mL<sup>-1</sup> (AgNP) against the pathogenic strain of *E.coli* was 16.2 mm (inhibition zone), 50 μg.mL<sup>-1</sup> (AgNP) was 20.4 mm, 90 μg.mL<sup>-1</sup> (AgNP) was 26.5 mm and 110 μg.mL<sup>-1</sup> (AgNP) was 31.3 mm (Fig. 5A), while antibacterial activity of 30 μg.mL<sup>-1</sup> (AgNP) against the pathogenic strain of *Klebsiella pneumonia* was 16 mm (inhibition zone), 50 μg.mL<sup>-1</sup> (AgNP) was 18.8 mm, 90 μg.mL<sup>-1</sup> (AgNP) was 26.5 mm and 110 μg.mL<sup>-1</sup> (AgNP) was 30.9 mm (Fig. 5B). The antibacterial activity of 30 μg.mL<sup>-1</sup> (AgNP) against the pathogenic strain of *Pseudomonas aeruginosa* was 16 mm (inhibition zone), 50 μg.mL<sup>-1</sup> (AgNP) was 18.8 mm, 90 μg.mL<sup>-1</sup> (AgNP) was 26.5 mm and 110 μg.mL<sup>-1</sup> (AgNP) was 30.9 mm (Fig. 5C). The antibacterial activity of 30 μg.mL<sup>-1</sup> (AgNP) against the pathogenic strain of *Proteus merabilis* was 16.9 mm (inhibition zone), 50 μg.mL<sup>-1</sup> (AgNP) was 20.4 mm, 90 μg.mL<sup>-1</sup>

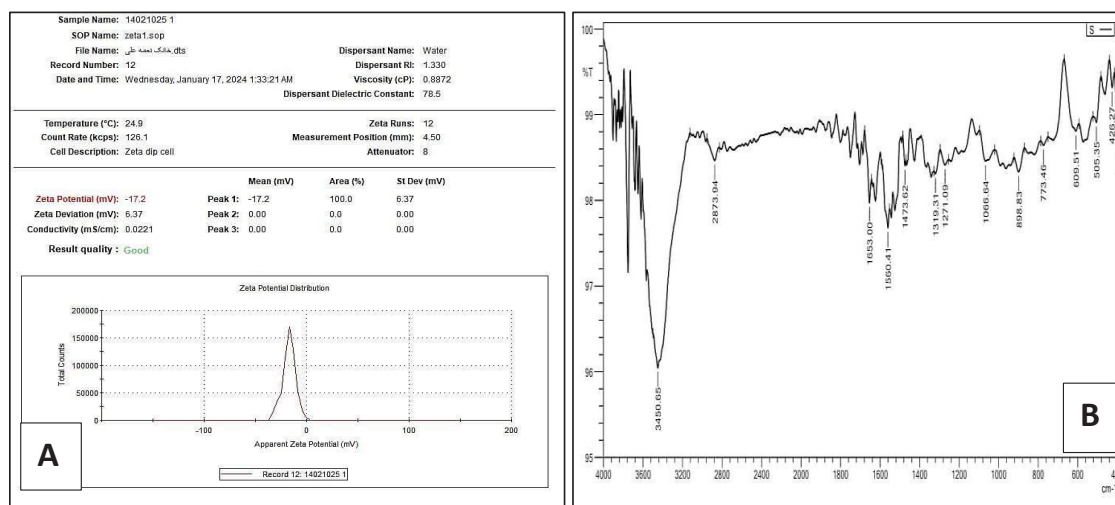


Fig. 4. Characterization of silver nanoparticles A: zeta potential B: fourier transform infrared spectroscopy (FTIR).

Table 2. Antibacterial activity of AgNPs against pathogenic strain (inhibition zone diameter in (mm)).

Bacterial strain	Inhibition zone (mm) by (30 μg.mL <sup>-1</sup> AgNP)	Inhibition zone (mm) by (50 μg.mL <sup>-1</sup> AgNP)	Inhibition zone (mm) by (90 μg.mL <sup>-1</sup> AgNP)	Inhibition zone (mm) by (110 μg.mL <sup>-1</sup> AgNP)
<i>E. coli</i>	16.2	20.4	26.5	31.3
<i>Klebsiella pneumonia</i>	16	18.8	26.5	30.9
<i>Pseudomonas aeruginosa</i>	16	18.8	26.5	30.9
<i>Proteus mirabilis</i>	16.9	20.4	26.3	30.4
<i>Staphylococcus aureus</i>	18.17	21.5	30.17	33.67
<i>Enterococcus faecalis</i>	17.8	23.4	31	34.6

(AgNP) was 26.3 mm and 110  $\mu\text{g mL}^{-1}$  (AgNP) was 30.4 mm (Fig. 5D). The antibacterial activity of 30  $\mu\text{g mL}^{-1}$  (AgNP) against the pathogenic strain of *Staphylococcus aureus* was 18.17 mm (inhibition zone), 50  $\mu\text{g mL}^{-1}$  (AgNP) was 21.5 mm, 90  $\mu\text{g mL}^{-1}$  (AgNP) was 30.17 mm and 110  $\mu\text{g mL}^{-1}$  (AgNP) was 33.67 mm (Fig. 5E). The antibacterial activity of 30  $\mu\text{g mL}^{-1}$  (AgNP) against the pathogenic strain of *Enterococcus faecalis* was 17.8 mm (inhibition zone), 50  $\mu\text{g mL}^{-1}$  (AgNP) was 23.4 mm, 90  $\mu\text{g mL}^{-1}$  (AgNP) was 31 mm and 110  $\mu\text{g mL}^{-1}$  (AgNP) was 34.6 mm (Fig. 5F).

The results of minimum inhibitory concentration (MIC) and minimum bactericidal concentration (MBC) ( $\mu\text{g mL}^{-1}$ ) of AgNPs for the pathogenic *E. coli* bacteria was 30 and 90 respectively. The results of minimum inhibitory concentration (MIC) and minimum bactericidal concentration (MBC) ( $\mu\text{g mL}^{-1}$ ) of AgNPs for the pathogenic *Klebsiella pneumoniae* bacteria was 50 and 110 respectively. The results of minimum inhibitory concentration (MIC) and minimum bactericidal concentration (MBC) ( $\mu\text{g mL}^{-1}$ ) of AgNPs for the pathogenic *Pseudomonas aeruginosa* bacteria was 50 and 110

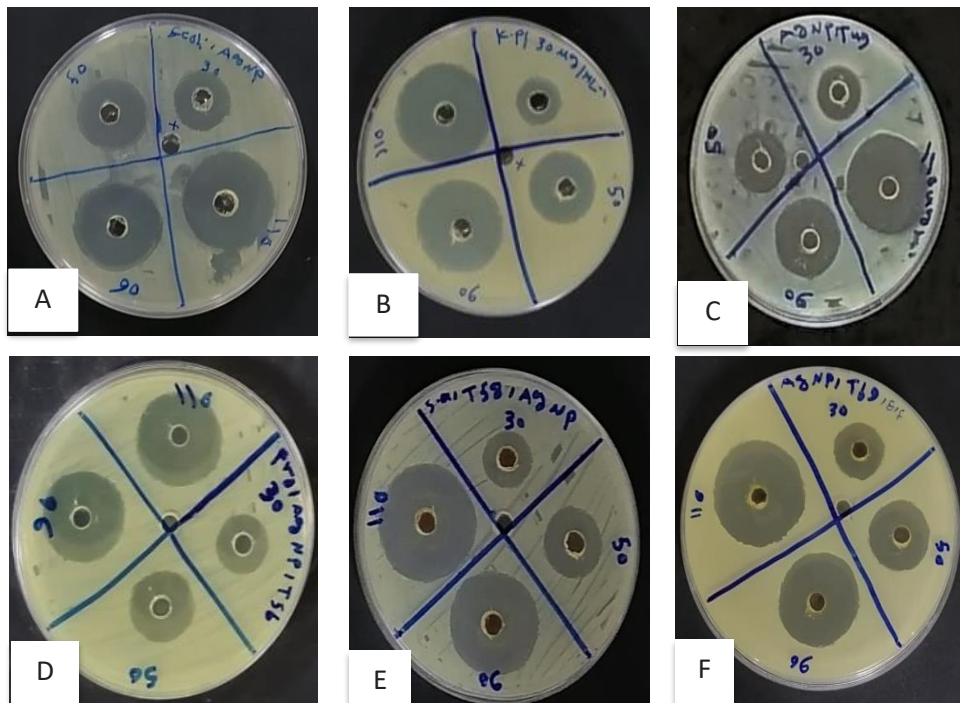


Fig. 5. Antibacterial activity of AgNPs against pathogenic strain (A): *E. coli*, (B): *Klebsiella pneumoniae*, (C): *Pseudomonas aeruginosa* (D): *Proteus mirabilis* (E): *Staphylococcus aureus* (F): *Enterococcus faecalis*.

Table 3. Preparation of MIC and MBC concentration ( $\mu\text{g mL}^{-1}$ ) of AgNPs for pathogenic bacteria.

Bacteria isolates	MIC	MBC
<i>E. coli</i>	30	90
<i>Klebsiella pneumoniae</i>	50	110
<i>Pseudomonas aeruginosa</i>	50	110
<i>Proteus mirabilis</i>	50	110
<i>Staphylococcus aureus</i>	30	90
<i>Enterococcus faecalis</i>	30	90

respectively. The results of minimum inhibitory concentration (MIC) and minimum bactericidal concentration (MBC) ( $\mu\text{g mL}^{-1}$ ) of AgNPs for the pathogenic *Proteus mirabilis* bacteria was 50 and 110 respectively. The results of minimum inhibitory concentration (MIC) and minimum bactericidal concentration (MBC) ( $\mu\text{g mL}^{-1}$ ) of AgNPs for the pathogenic *Staphylococcus aureus* bacteria was 30 and 90 respectively. The results of minimum inhibitory concentration (MIC) and minimum bactericidal concentration (MBC) ( $\mu\text{g mL}^{-1}$ ) of AgNPs for the pathogenic *Enterococcus faecalis* bacteria was 30 and 90 respectively, as shown in Table 3.

The results in Table 4 showed that all the pathogenic bacteria in this study formed strong biofilm when no AgNP was added to the media. The results of minimum inhibitory concentration (MIC) against pathogenic biofilm forming bacterial strains of *E. coli* of 50  $\mu\text{g mL}^{-1}$  showed no biofilm growth in 17 (100%), while against pathogenic biofilm forming bacterial strains of *E. coli* of 30  $\mu\text{g mL}^{-1}$  showed weak biofilm growth in 17 (100%) and *E. coli* without AgNPs was strong biofilm growth 17 (100%). The results of minimum inhibitory concentration (MIC) against pathogenic biofilm forming bacterial strains of *Klebsiella pneumonia* of 50  $\mu\text{g mL}^{-1}$  showed no biofilm growth in 19 (100%), while against pathogenic biofilm forming bacterial strains of *Klebsiella pneumonia* of 30  $\mu\text{g mL}^{-1}$  showed no biofilm growth in 7 (36.84%) and weak growth of biofilm in 12 (63.16%), but *Klebsiella pneumonia* without AgNPs showed strong biofilm growth in 19 (100%). The results of minimum inhibitory concentration (MIC) against pathogenic biofilm forming bacterial strains of *Pseudomonas aeruginosa* of 50  $\mu\text{g mL}^{-1}$  showed no biofilm growth in 16 (100%), while against pathogenic biofilm forming bacterial strains of *Pseudomonas aeruginosa* of 30  $\mu\text{g mL}^{-1}$  showed no biofilm growth in 5 (31.25%) and weak biofilm growth in 11 (68.75%), while *Pseudomonas aeruginosa* without AgNPs showed strong biofilm growth in 16 (100%). The results of minimum inhibitory concentration (MIC) against pathogenic biofilm forming bacterial strains of *Proteus mirabilis* of 50  $\mu\text{g mL}^{-1}$  showed no biofilm formation in 5 (55.56%) and weak biofilm growth in 4 (44.44%), while against pathogenic biofilm forming bacterial strains of *Proteus mirabilis* of 30  $\mu\text{g mL}^{-1}$  showed weak biofilm growth in 9 (100%), and MIC against *Proteus mirabilis* without AgNPs showed strong

biofilm growth in 9 (100%). The results of minimum inhibitory concentration (MIC) against pathogenic biofilm forming bacterial strains of *Staphylococcus aureus* of 50  $\mu\text{g mL}^{-1}$  showed weak biofilm growth in 9 (100%), while against pathogenic biofilm forming bacterial strains of *Staphylococcus aureus* of 30  $\mu\text{g mL}^{-1}$  showed weak biofilm growth in 9 (100%), and MIC against *Staphylococcus aureus* without AgNPs showed strong biofilm growth in 9 (100%). The results of minimum inhibitory concentration (MIC) against pathogenic biofilm forming bacterial strains of *Enterococcus faecalis* of 50  $\mu\text{g mL}^{-1}$  showed weak biofilm growth in 5 (100%), while against pathogenic biofilm forming bacterial strains of *Enterococcus faecalis* of 30  $\mu\text{g mL}^{-1}$  showed weak biofilm growth in 5 (100%), and MIC against *Enterococcus faecalis* without AgNPs was strong biofilm growth in 5 (100%), as illustrated in Table 4 and Fig. 6.

Urinary tract infections (UTIs) are caused by a variety of different bacteria, which differs depending on the patient's resistance, and the type of infection with these microorganisms [18]. The most common etiologic agents isolated from the urinary system are enteric Gram-negative rods, Gram-positive bacteria, and some fungi [19]. Although our results showed that *Klebsiella pneumoniae* was the most prevalent bacteria causing UTI followed by *Escherichia coli*, most studies revealed that *Escherichia coli* was the major causative agent of UTI followed by *Klebsiella pneumoniae*, and this may be due to the small sample size in our study, which may not show a true impression of the bacterial types. In a study conducted by [20], they found that the most prevalent bacteria was *Escherichia coli* followed by *Klebsiella pneumonia* then *Pseudomonas aeruginosa*, *Staphylococcus aureus*, *Proteus mirabilis*, then *Enterococcus spp.* with variations in their sequence of prevalence.

The results in the current study revealed that clear antibacterial activity of (AgNP) against the pathogenic strains of the six bacterial types was shown, and the inhibition diameter increased with increasing the concentration of AgNP concentrations.

In several previous studies, AgNPs have been exposed to the strains of *S. aureus*, *E. faecalis*, *E. coli*, *P. mirabilis*, *K. pneumoniae*, and *P. aeruginosa*. They specifically describe that a binding and penetration of AgNPs into the bacterial membrane was observed through the destruction of the cell

wall; likewise, some reactions occurred with the thiol groups (-SH) of proteins, and finally, DNA replication was prevented, causing bacterial death [21].

Nano-particles can exert their antibacterial activity through many mechanisms, such as: (1) direct interaction with the bacterial cell wall; (2) inhibition of biofilm formation; (3) triggering the innate and adaptive host immune responses; (4) generation of reactive oxygen species (ROS); and (5) induction of intracellular effects leading to apoptosis (e.g. interactions with DNA and/or proteins) [22].

The results of minimum inhibitory concentration

(MIC) against biofilm forming for pathogenic bacteria strains of each of (*E.coli*, *Klebsiella pneumoniae*, *Pseudomonas aeruginosa*, *Proteus mirabilis*, *Saphylococcus aureus* and *Enterococcus faecalis*) of 50  $\mu\text{g.mL}^{-1}$  showed none biofilm growth and shown weak biofilm growth of the bacteria strains, while 30  $\mu\text{g.mL}^{-1}$  showed none and weak biofilm growth, while without AgNPs was strong biofilm growth of the every bacteria strains, and concentration of 50  $\mu\text{g.mL}^{-1}$  shown higher effect from concentration of 30  $\mu\text{g.mL}^{-1}$  on biofilm formation, and AgNPs (MIC) shown more effective against biofilm of Gram negative bacteria than Gram positive bacteria.

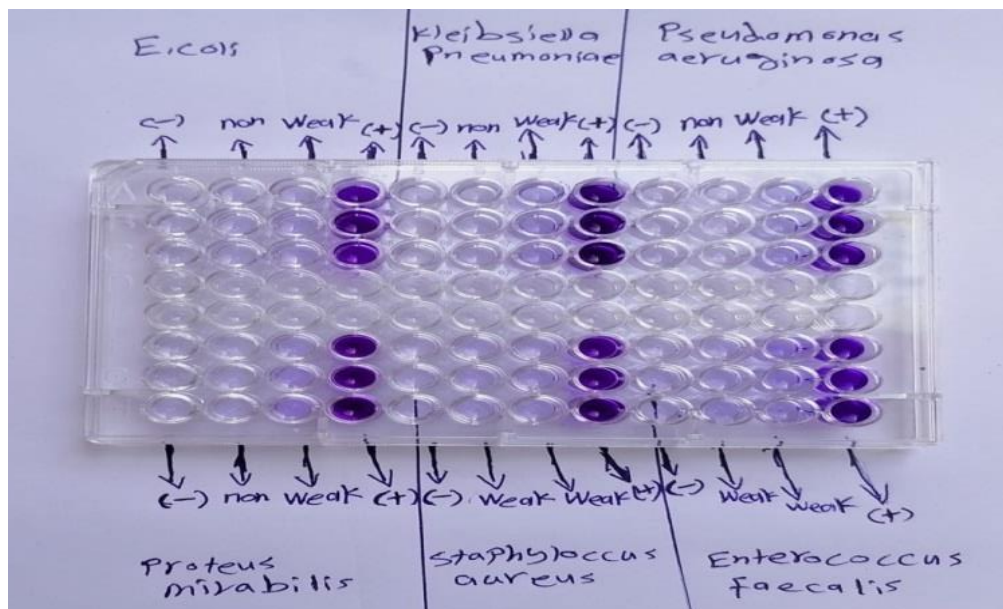


Fig. 6. Result of AgNP effect on biofilm forming for pathogenic bacteria strains by ELISA using microtiter plate 96 wells.

Table 4. Anti-biofilm effect of AgNPs (MIC) (50 and 30  $\mu\text{g. mL}^{-1}$ ) against biofilm forming by pathogenic bacteria strains using microtiter plate 96 wells.

Treatment Bacteria strain	AgNPs (50 $\mu\text{g.mL}^{-1}$ )	AgNPs (30 $\mu\text{g.mL}^{-1}$ )	Without AgNPs
<i>E. coli</i>	None 17 (100%)	Weak 17 (100%)	Strong 17 (100)
<i>Klebsiella pneumoniae</i>	None 19 (100%)	None 7 (36.84%) Weak 12 (63.16%)	Strong 19 (100%)
<i>Pseudomonas aeruginosa</i>	None 16 (100%)	None 5 (31.25%) Weak 11 (68.75%)	Strong 16 (100%)
<i>Proteus mirabilis</i>	None 5 (55.56%) Weak 4 (44.44%)	Weak 9 (100%)	Strong 9 (100%)
<i>Staphylococcus aureus</i>	Weak 9 (100%)	Weak 9 (100%)	Strong 9 (100%)
<i>Enterococcus faecalis</i>	Weak 5 (100%)	Weak 5 (100%)	Strong 5 (100%)

Bacterial resistance to antibiotics and the potential to colonize abiotic surfaces through the formation of biofilm are major causes of medical implant-associated infections, leading to prolonged hospital stays and patient mortality. Various strategies have been adopted in medical settings to prevent biofilm-associated infections [23].

A study performed by [24] reported that seven different silver nanoparticles concentrations were tested for their antimicrobial activities. Also, anti-biofilm activities against *E. coli* U12 were tested. Using the dilution method, the silver nanoparticles concentration of 85 µg/ml was the MIC (Minimum Inhibitory Concentration) that had excellent biocompatibility and showed significant antibacterial activity against *E. coli* U12.

One of the main mechanisms that nanoparticles present when interacting with biofilms generated by bacteria is the interaction with EPS, which will allow the access of any chemical molecule agentive to the bacteria and, thus, cause damage to the cell [25,26]. It has also been reported that NPs in contact with bacteria can affect the bacterial adhesion rate causing damage to biofilms, which is attributed to metabolic inhibition processes by releasing metal ions; however, the specific mechanisms cannot yet be fully explained [21].

Other factors related to the NPs also contribute to the antibiofilm action of NPs, such as hydrophobicity, shape, and surface charge [27]. Carefully considering these factors when designing anti-biofilm NPs can aid the synthesis of NPs targeting bacterial biofilms. To destroy the bacteria inside the biofilm, NPs may inflict an antimicrobial action directly or deliver therapeutic agents, such as antibiotics or antimicrobials (e.g. essential oils, enzymes, or phytochemicals) [28].

Another anti-biofilm mechanism of silver NPs is integrating within the bacterial DNA and causing damage [29].

## CONCLUSION

This study demonstrates the significant antibacterial and anti-biofilm efficacy of silver nanoparticles (AgNPs) against common bacterial strains causing urinary tract infections (UTIs). The results revealed a clear correlation between AgNP concentration and bacterial inhibition, with higher concentrations exhibiting stronger inhibitory effects. AgNPs successfully disrupted biofilm formation and reduced bacterial growth

in vitro, highlighting their potential as an effective antimicrobial agent against persistent biofilm-associated infections. The findings also confirmed that AgNPs penetrate bacterial membranes, disrupt cell walls, and inhibit critical processes such as DNA replication, leading to bacterial death. These results underscore the promise of AgNPs as a novel therapeutic approach for managing UTIs, particularly those complicated by biofilm-forming bacteria. Further studies are warranted to optimise the application of AgNPs in clinical settings and assess their long-term safety and efficacy. This research contributes to the growing body of evidence supporting nanoparticle-based solutions for combating antibiotic-resistant infections.

## CONFLICT OF INTEREST

The authors declare that there is no conflict of interest regarding the publication of this manuscript.

## REFERENCES

1. Ali MA, Alkhafaji MH. Antibiofilm Activity of Biosynthesized Enterococcus-Iron Oxide Nanoparticles against Uropathogenic Bacteria. *Egyptian Journal of Botany*. 2022.
2. Odoki M, Almustapha Aliero A, Tibyangye J, Nyabayo Maniga J, Wampande E, Drago Kato C, et al. Prevalence of Bacterial Urinary Tract Infections and Associated Factors among Patients Attending Hospitals in Bushenyi District, Uganda. *Int J Microbiol*. 2019;2019:1-8.
3. Bharadwaj KK, Rabha B, Choudhury BK, Rosalin R, Sarkar T, Baishya D, et al. Current strategies in inhibiting biofilm formation for combating urinary tract infections: Special focus on peptides, nano-particles and phytochemicals. *Biocatalysis and Agricultural Biotechnology*. 2021;38:102209.
4. Patra JK, Das G, Fraceto LF, Campos EVR, Rodriguez-Torres MdP, Acosta-Torres LS, et al. Nano based drug delivery systems: recent developments and future prospects. *Journal of Nanobiotechnology*. 2018;16(1).
5. Bruna T, Maldonado-Bravo F, Jara P, Caro N. Silver Nanoparticles and Their Antibacterial Applications. *Int J Mol Sci*. 2021;22(13):7202.
6. Ashwak Jasim K. Antimicrobial and Biofilm Inhibitory Activity of Nanoparticles Against Clinical Isolates from Urinary Tract Infection. *Indian Journal of Forensic Medicine and Toxicology*. 2020;14(3):194-199.
7. Hayat S. Nanoantibiotics Future nanotechnologies to combat antibiotic resistance. *Front Biosci*. 2018;10(2):352-374.
8. Pinzaru I, Coricovac D, Dehelean C, Moacă E-A, Mioc M, Baderca F, et al. Stable PEG-coated silver nanoparticles – A comprehensive toxicological profile. *Food and Chemical Toxicology*. 2018;111:546-556.
9. Kwakman PHS, de Boer L, Ruyter-Spira CP, Creemers-Molenaar T, Helsper JPF, Vandenbroucke-Grauls CMJE, et al. Medical-grade honey enriched with antimicrobial peptides has enhanced activity against antibiotic-resistant

- pathogens. *European Journal of Clinical Microbiology & Infectious Diseases*. 2010;30(2):251-257.
10. Ibraheem DR, Hussein NN, Sulaiman GM. Antibacterial Activity of Silver nanoparticles Against Pathogenic Bacterial Isolates from Diabetic Foot Patients. *Iraqi Journal of Science*. 2023;2223-2239.
  11. Talar Ibrahim H, Akhter Ahmed A. Characterization, antibacterial and antibiofilm evaluation of biosynthesized silver nanoparticles from *Pseudomonas aeruginosa* against drug resistant *Acinetobacter baumannii*. *Al Mustansiriyah Journal of Pharmaceutical Sciences*. 2023;23(3):307-321.
  12. Abdulazeem L, Abdalkareem Jasim S, Rajab WJ. WITHDRAWN: Anti-bacterial activity of gold nanoparticles against two type of antibiotic resistance pathogenic bacteria in Al-Hilla city. *Materials Today: Proceedings*. 2021.
  13. Johansen FR. Toxicological profile of carboxymethyl inulin. *Food and Chemical Toxicology*. 2003;41(1):49-59.
  14. Zhang X-F, Liu Z-G, Shen W, Gurunathan S. Silver Nanoparticles: Synthesis, Characterization, Properties, Applications, and Therapeutic Approaches. *Int J Mol Sci*. 2016;17(9):1534.
  15. Biosynthesis Silver Nanoparticles and Assessment of Antibacterial Activity Against to some type of pathogenic bacteria. *Humanitarian and Natural Sciences Journal*. 2024;5(6).
  16. Mfon RE, Labulo AH, Al Amri Z, Esaduwha S, Labaran J. Effect of Carbon Nanotubes on the performance of Perovskite Solar Cells. *European Journal of Energy Research*. 2022;2(4):62-68.
  17. An Investigation of Green Synthesis of Silver Nanoparticles Using Turkish Honey Against Pathogenic Bacterial Strains. *Biointerface Research in Applied Chemistry*. 2022;13(2):195.
  18. Kot B. Antibiotic Resistance Among Uropathogenic *Escherichia coli*. *Polish Journal of Microbiology*. 2019;68(4):403-415.
  19. Isa SA, Mustapha Y K, Hamza A J, Rashida S. Evaluation of The Incidence of Uropathogenic Bacteria Among Pregnant Women Attending Antenatal Clinic Doma Hospital Gombe. *Bima Journal of Science and Technology (2536-6041)*. 2022;6(03):129-135.
  20. Muna FJ, Mohammed Hashim ALY. Microbial Infections Associated with Diabetic Foot Ulcer in Nasiriyah City. *Indian Journal of Forensic Medicine & Toxicology*. 2021;15(2):2887-2892.
  21. Balderrama-González A-S, Piñón-Castillo H-A, Ramírez-Valdespino C-A, Landeros-Martínez L-L, Orrantia-Borunda E, Esparza-Ponce H-E. Antimicrobial Resistance and Inorganic Nanoparticles. *Int J Mol Sci*. 2021;22(23):12890.
  22. Eltarahony M, Zaki S, Abd-El-Haleem D. Concurrent Synthesis of Zero- and One-Dimensional, Spherical, Rod-, Needle-, and Wire-Shaped CuO Nanoparticles by *Proteus mirabilis* 10B. *Journal of Nanomaterials*. 2018;2018:1-14.
  23. Li X, Fan H, Zi H, Hu H, Li B, Huang J, et al. Global and Regional Burden of Bacterial Antimicrobial Resistance in Urinary Tract Infections in 2019. *Journal of Clinical Medicine*. 2022;11(10):2817.
  24. Selem E, Mekky AF, Hassanein WA, Reda FM, Selim YA. Antibacterial and antibiofilm effects of silver nanoparticles against the uropathogen *Escherichia coli* U12. *Saudi J Biol Sci*. 2022;29(11):103457.
  25. Niño-Martínez N, Salas Orozco MF, Martínez-Castañón G-A, Torres Méndez F, Ruiz F. Molecular Mechanisms of Bacterial Resistance to Metal and Metal Oxide Nanoparticles. *Int J Mol Sci*. 2019;20(11):2808.
  26. Salas-Orozco M, Niño-Martínez N, Martínez-Castañón G-A, Méndez FT, Jasso MEC, Ruiz F. Mechanisms of Resistance to Silver Nanoparticles in Endodontic Bacteria: A Literature Review. *Journal of Nanomaterials*. 2019;2019:1-11.
  27. Al-Wrafy FA, Al-Gheethi AA, Ponnusamy SK, Noman EA, Fattah SA. Nanoparticles approach to eradicate bacterial biofilm-related infections: A critical review. *Chemosphere*. 2022;288:132603.
  28. Lin Y-K, Yang S-C, Hsu C-Y, Sung J-T, Fang J-Y. The Antibiofilm Nanosystems for Improved Infection Inhibition of Microbes in Skin. *Molecules*. 2021;26(21):6392.
  29. Mao B-H, Chen Z-Y, Wang Y-J, Yan S-J. Silver nanoparticles have lethal and sublethal adverse effects on development and longevity by inducing ROS-mediated stress responses. *Sci Rep*. 2018;8(1).